

# Formability of YAG Laser Welded TRIP-aided Dual-phase Steel Sheets\*

Akihiko NAGASAKA,\*\* Atsushi MIO,\*\*\* Kazuhide WADA\*\*\* and Masakatsu SAITO\*\*\*

The effects of YAG laser welding conditions on mechanical properties and press formability (bendability, stretch-formability and deep drawability) of high strength TRIP-aided dual-phase (TDP) steel were investigated. Tensile tests and press forming tests have been conducted for laser butt welded joints obtained from the combination of the same steel. The tensile property and press formability were affected by the welding speed of 100 to 1100 mm/min and the energy of 5 to 9 J/pulse. The excellent press formability was obtained by using the energy of 6 J/pulse and the welding speed of 300 mm/min. It was concluded that the excellent weldability of the TDP steel was ascribed to the weld joints formation.

Key words: YAG laser welding, retained austenite, transformation-induced plasticity.

## 1. Introduction

Dual-phase steel associated with the transformation-induced plasticity (TRIP)[1] of the retained austenite ( $\gamma_R$ ), or TDP steel, possesses the excellent press formability of high-strength sheet steels which were recently developed for shock safety and weight reduction of the automobile.[2–5] Hence, much research has been conducted to apply the steel to various automotive structural parts such as impact-prone parts and suspension parts.[6] The press formability of the TDP steel is expected to be controlled by the retained austenite parameters (volume fraction, carbon concentration and morphology), in the same ways as elongation[7–10], stretch-formability[11, 12] and stretch-flangeability.[13–15] The tailored blank method has been applied for steel sheet welded structures.[16] However, there have been few investigations dealing with the tailored blank from such a point of view.

In this study, joint test specimens, all manufactured from the same materials, on which butt welding was performed using a YAG laser, were fabricated. In order to clarify the laser process conditions required to form TDP steel, tensile properties and press formability were investigated.

## 2. Experimental Procedure

An as-cold-rolled sheet steel with the chemical composition of 0.20C–1.51Si–1.51Mn (mass%) 1.2 mm in thickness used in this study is shown in Table 1. The

Table 1. Chemical composition of steels used (mass%).

Steel	C	Si	Mn	P	S	Al
TDP	0.20	1.51	1.51	0.015	0.0011	0.040
MDP	0.14	0.21	1.74	0.013	0.0030	0.037

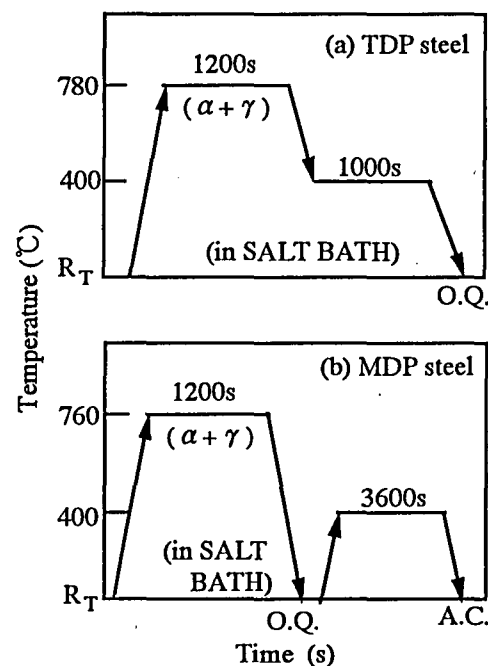


Fig. 1. Heat treatment diagram of TDP and MDP steels, in which "O.Q." and "A.C." represent quenching in oil and air cooling, respectively.

\* Retouch correction of SISE '2001; July 31 — August 2, 2001

\*\* Associate Professor, Department of Mechanical Engineering

\*\*\* First Technical Section

Received October 28, 2001

TDP steel was intercritically annealed, and was austempered in salt baths, as shown in Fig. 1(a). For comparison, 0.14C – 0.21Si – 1.74Mn (mass%) ferrite ( $\alpha_f$ ) – martensite ( $\alpha_m$ ) dual-phase steel (MDP steel) subjected to heat treatment shown in Fig. 1(b), was also prepared.

For butt welding, the blank obtained after the heat treatment was cut using a fine cutter, and YAG laser processing equipment (pulse oscillation, maximum average output of 350 W, maximum peak output of 4.5 kW) was used. The processing conditions were as follows. Pulse energy ( $E$ ) and welding speed ( $F$ ) were varied;  $E=6$  and 9 J/P, and  $F=100-1100$  mm/min. The pulse width was constant at 3.8 ms, and the material was shielded by  $N_2$  gas.

Tensile tests were performed on an Instron tensile testing machine at a crosshead speed of 1 mm/min (strain rate  $2.8 \times 10^{-4}$  /s), using JIS-13B-type tensile specimens. The press formability was evaluated from the minimum bending radius ( $R_{min}$ ), the maximum stretch-height ( $H_{max}$ ) [12] and the limiting drawing ratio ( $LDR$ ), [5] The laser-irradiated side was made convex.

The volume fraction of the retained austenite was quantified by X-ray diffractometry using Mo-K $\alpha$  radiation (five-peak method). [17] In addition, the initial carbon concentration in the retained austenite ( $C_{\gamma 0}$ , mass%) was estimated from the lattice parameter ( $a_{\gamma 0}$ , nm) measured from the (220) $\gamma$  diffraction peak of Cr-K $\alpha$  radiation using the following equation. [18]

$$C_{\gamma 0} = (a_{\gamma 0} - 0.35467) / 4.67 \times 10^{-3} \cdot \dots \cdot (1)$$

### 3. Results and Discussion

#### 3.1. Structure and tensile properties

Figure 2 shows optical and scanning electron micrographs of the TDP steel, in which white phases in (a) represent the retained austenite. The optical micrograph was color etched using the LePare method while the scanning electron micrograph was etched in a 3% nital solution. The retained austenite and bainite ( $\alpha_b$ ) phases as the hard second phase lie along the ferrite grain boundary. An initial volume fraction ( $f_{\gamma 0}$ ), and an initial carbon concentration ( $C_{\gamma 0}$ ) of the retained austenite in TDP steel were 9 vol% and 1.38 mass%, respectively (Table 2). TDP steel presents a higher  $n$ -value compared to MDP steel, however, the  $r$ -value of TDP steel was low at less than 1.0, similar to that of MDP steel.

#### 3.2. Tensile properties after welding

Figure 3 shows the relationship between tensile strength ( $TS$ ) and welding speed ( $F$ ), and the relationship between total elongation ( $TEI$ ) and welding speed ( $F$ ). Total elongation of TDP steel was at a maximum for  $F=200-400$  mm/min at both pulse energies, which was the same for conventional total elongation. MDP steel presented a similar tendency, although approximately 10% total elongation was obtained.

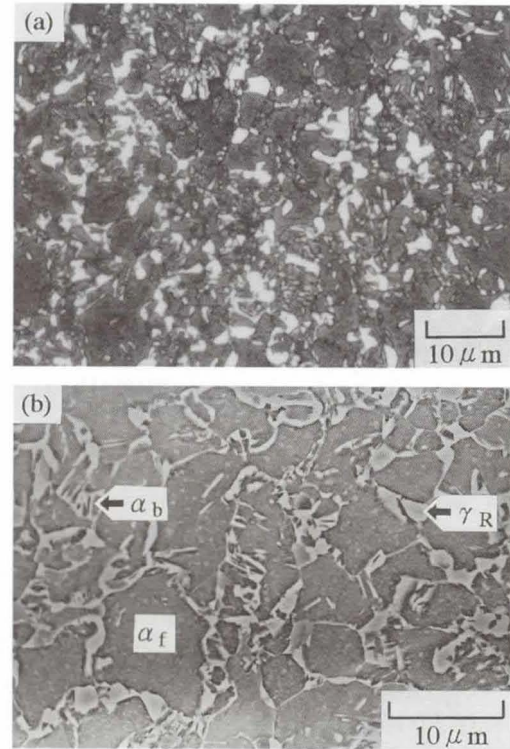


Fig. 2. Optical and scanning electron micrographs of TDP steel, in which white phases represent retained austenite and " $\alpha_f$ ", " $\alpha_b$ " and " $\gamma_R$ " are ferrite matrix, bainite island and retained austenite particle, respectively.

Table 2. Retained austenite characteristics and tensile properties.

Steel	$f$	$f_{\gamma 0}$	$C_{\gamma 0}$ (mass%)	$TS$ (MPa)	$TEI$ (%)	$n$	$r$
TDP	0.35	0.09	1.38	825	36.0	0.26	0.72
MDP	0.27	-	-	788	12.5	0.08	0.80

$f$ : volume fraction of second phase,  $f_{\gamma 0}$ : initial volume fraction of retained austenite,  $C_{\gamma 0}$ : initial carbon concentration in retained austenite,  $TS$ : tensile strength,  $TEI$ : total elongation,  $n$ : work hardening exponent and  $r$ :  $r$ -value.

Figure 4 shows an example of the appearance of the fractured tensile test specimen ( $E=6 \text{ J/P}$ ). The specimen in (a), when  $F=300 \text{ mm/min}$ , was fractured away from a weld joint, while the specimen in (b), when  $F=500 \text{ mm/min}$ , was fractured at a weld joint. Accordingly, obtaining total elongation equal to the conventional total elongation indicated that the joint was in good condition.

Figure 5 shows a sample of the cross section of a weld joint, 3% of which was etched by nital ( $E=9 \text{ J/P}$ ,  $F=900 \text{ mm/min}$ ). The white area in the middle of the image was completely transformed to  $\alpha_m$  and the black area was a heat-affected zone (HAZ). Penetration of a bead was completely achieved in the form of a V shape, resulting in a decrease in the thickness of the bead ( $t$ ) compared to the thickness of the sheet ( $t_0$ ). The lower the welding speed, the greater the rectangular penetration and the larger the area transformed to  $\alpha_m$  and HAZ.

Figure 6 shows the relationship between the thickness ratio ( $t/t_0$ ) of the thickness of the completely penetrated bead ( $t$ ) to the thickness of the sheet ( $t_0$ ) and welding speed ( $F$ ).

Figure 7 shows the distribution of Vickers hardness  $HV$  (load 0.98 N) from the center of a weld joint. As a standard to determine the appropriateness of the bead shape,  $t/t_0 \geq 0.7$  is proposed, indicating that when  $t/t_0 < 0.7$ , rupture occurs at a weld joint, and when  $t/t_0 \geq 0.7$ , rupture occurs in the base metal. [16] A substantial decrease in total elongation shown in Fig. 3(b) occurring when  $E=6 \text{ J/P}$  and  $F > 300 \text{ mm/min}$  was attributed to incomplete joint penetration. When  $E=9 \text{ J/P}$ , total elongation decreased similarly, but since joint bead penetration was complete,

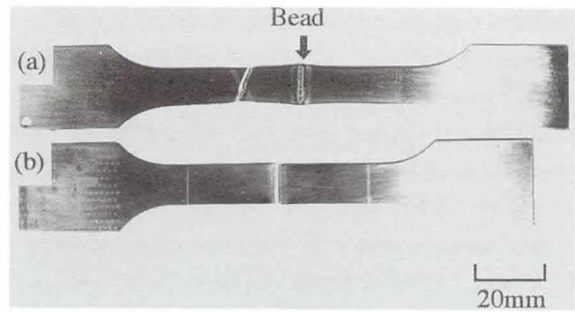


Fig. 4. Appearance of some specimens in TDP steel. (a)  $E=6 \text{ J/P}$ ,  $F=300 \text{ mm/min}$ , (b)  $E=6 \text{ J/P}$ ,  $F=500 \text{ mm/min}$ .

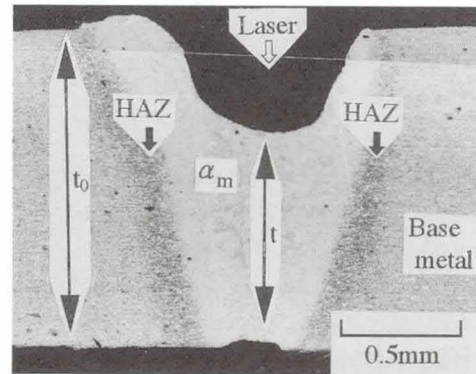


Fig. 5. Example of cross-section of YAG laser weld. ( $E=9 \text{ J/P}$ ,  $F=900 \text{ mm/min}$ )

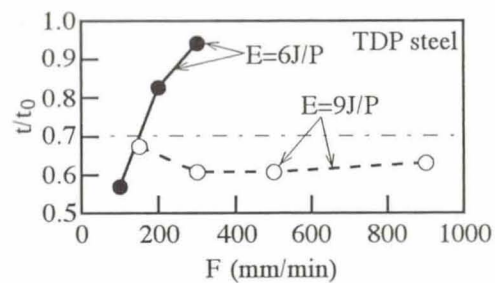


Fig. 6. Variation in welding thickness ratio ( $t/t_0$ ) as a function of welding speed ( $F$ ) in TDP steel.

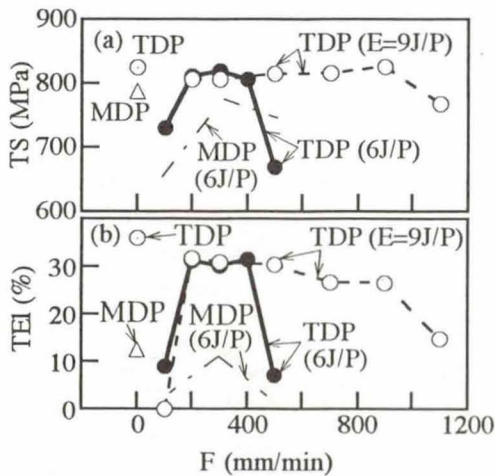


Fig. 3. Variations in (a) tensile strength ( $TS$ ) and (b) total elongation ( $TEI$ ) as a function of welding speed ( $F$ ) in TDP and MDP steels.

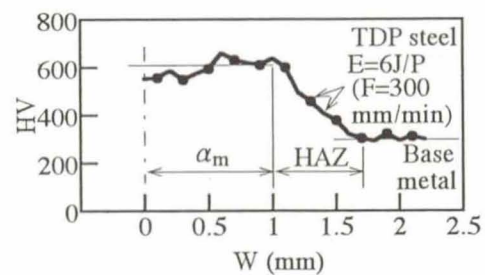


Fig. 7. Variation in Vickers hardness ( $HV$ ) at the cross section of distance from center of weld zone ( $W$ ) in TDP steel.

the rapid decrease in total elongation observed when  $E=6$  J/P was not observed. Meanwhile, in the range of low  $F$  ( $F < 200$  mm/min) when  $E=6$  J/P, burn through occurred in the base metal, and again  $t/t_0 < 0.7$  and the minimum cross-sectional area decreased, resulting in the promotion of regional deformation (Fig. 6). A  $n$ -value of 0.2 or greater across a weld joint was maintained, indicating a high work hardening exponent (Table 2); however, it is difficult to say whether good elongation can be consistently obtained because constraint of the base metal in the welding direction is high. As the reason for this, we considered that since the hardness ratio of a weld joint transformed to  $\alpha_m$  ( $HV600$ ) to the base metal ( $HV290$ ) was approximately two (Fig. 7), the constraint in the direction of the sheet width was increased.

### 3.3. Formability after welding

Figure 8 shows the relationship between the minimum bending radius ( $R_{min}$ ) and welding speed ( $F$ ). In Figs. 8(a) and (b), the laser irradiated surfaces were made face bend and root bend, respectively. Figure 9 shows the relationship between the maximum stretch-height ( $H_{max}$ ) and welding speed ( $F$ ), and the relationship between the limiting drawing ratio ( $LDR$ ) and welding speed ( $F$ ). In Fig. 8(a), when  $E=6$  J/P and  $F=300$  mm/min or greater,  $R_{min}$  was almost minimum and the bendability appeared to be good, while when  $E=9$  J/P,  $R_{min}$  was 5 mm or greater and the bendability was poor, i.e., fracture occurred. In Fig. 8(b), when  $E=6$  J/P and  $F=300$  mm/min,  $R_{min}$  was minimum. This was due to a change in shape of the laser surface induced when  $E=9$  J/P, which acted as a notch and caused concentration of stress. Meanwhile, the stretch formability and deep drawability decreased compared to the conventional  $H_{max}$  and  $LDR$ . As the reason for this, we considered that since the hardness ratio of a weld joint transformed to  $\alpha_m$  to the base metal was approximately two, stretching deformation was constrained to the weld joint when the surface area was expanded due to stretch forming, and the drawing resistance of the shrinking flange was constrained and increased by deep drawing. Accordingly, the optimal laser welding condition for forming TDP steel was found to be around  $F=300$  mm/min at  $E=6$  J/P.

## 4. Conclusions

The effects of YAG laser welding conditions on mechanical properties and press formability of high strength TRIP-aided dual-phase (TDP) steel were

investigated. The principle conclusions are summarized as follows.

- (1) The optimal laser welding conditions for forming TDP steel were found to be a pulse energy  $E=6$  J/P and a welding speed  $F=300$  mm/min.
- (2) The optimal condition was when bead penetration was completely achieved and the ratio of bead thickness  $t$  to sheet thickness  $t_0$  was  $t/t_0 \geq 0.7$ .

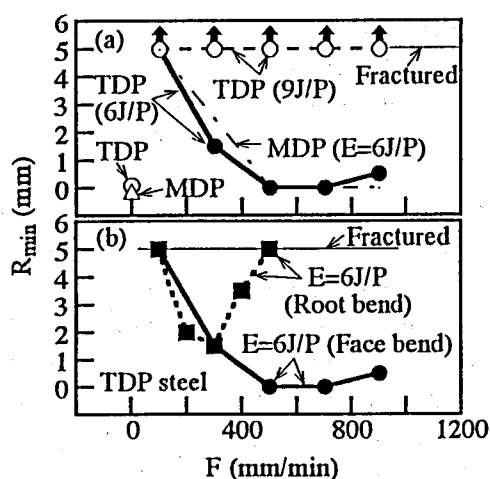


Fig. 8. Variation in minimum bending radius ( $R_{min}$ ) as a function of welding speed ( $F$ ) in TDP and MDP steels.

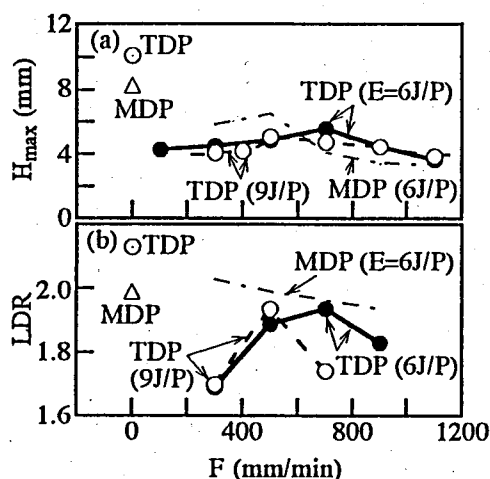


Fig. 9. Variations in (a) maximum stretch-height ( $H_{max}$ ) and (b) limiting drawing ratio ( $LDR$ ) as a function of welding speed ( $F$ ).

### Acknowledgements

The authors thank The Die and Mold Technology Promotion Foundation and The Amada Foundation for Metal Work Technology for their financial support. The authors would like to thank Mr. S. Kurumi, Mr. A. Nishiyama, Mr. K. Kuwano and Mr. M. Fujimaki, NNCT for their helpful discussions.

### References

- [1] V. F. Zackay, E. R. Parker, D. Fahr and R. Busch: *Trans. Am. Soc. Met.*, **60** (1967), 252.
- [2] O. Matsumura, T. Ohue and T. Amaike: *Tetsu-to-Hagane*, **79** (1993), 209.
- [3] S. Hiwatashi, M. Takahashi, T. Katayama and M. Usuda: *J. Jpn. Soc. Technol. Plast.*, **35** (1994), 1109.
- [4] A. Nagasaka, K. Sugimoto, M. Kobayashi and S. Hashimoto: *Tetsu-to-Hagane*, **85** (1999), 552.
- [5] A. Nagasaka, K. Sugimoto, M. Kobayashi, Y. Kobayashi and S. Hashimoto: *Tetsu-to-Hagane*, **87** (2001), 607.
- [6] Y. Ojima, Y. Shiroy, Y. Taniguchi and K. Kato: *SAE Tech. Pap. Ser.*, #980954, (1998), 39.
- [7] O. Matsumura, Y. Sakuma and H. Takechi: *Trans. Iron Steel Inst. Jpn.*, **27** (1987), 570.
- [8] K. Sugimoto, M. Kobayashi and S. Hashimoto: *Metall. Trans. A*, **23A** (1992), 3085.
- [9] K. Sugimoto, N. Usui, M. Kobayashi and S. Hashimoto: *ISIJ Int.*, **32** (1992), 1311.
- [10] K. Sugimoto, M. Misu, M. Kobayashi and H. Shirasawa: *ISIJ Int.*, **33** (1993), 775.
- [11] O. Matsumura, Y. Sakuma, Y. Ishii and J. Zhao: *ISIJ Int.*, **32** (1992), 1110.
- [12] K. Sugimoto, M. Kobayashi, A. Nagasaka and S. Hashimoto: *ISIJ Int.*, **35** (1995), 1407.
- [13] A. Nagasaka, K. Sugimoto, M. Kobayashi and S. Hashimoto: *Tetsu-to-Hagane*, **83** (1997), 335.
- [14] A. Nagasaka, K. Sugimoto, M. Kobayashi and H. Shirasawa: *Tetsu-to-Hagane*, **84** (1998), 218.
- [15] K. Sugimoto, A. Nagasaka, M. Kobayashi and S. Hashimoto: *ISIJ Int.*, **39** (1999), 56.
- [16] K. Kubota: *J. Soc. Automo. Engrs. Jpn.*, **50** (1996), 17.
- [17] H. Maruyama: *J. Jpn. Soc. Heat Treat.*, **17** (1977), 198.
- [18] Z. Nishiyama: *Martensite Transformation*, Maruzen, Tokyo, (1971), 13.